Research article

A screen-printed electrode modified with gold nanoparticles/cellulose nanocrystals for electrochemical detection of 4,4′-methylene diphenyl diamine

Duygu Büyüktaş [a,b], Masoud Ghaani [b], Cesare Rovera [b], Daniele Carullo [b], Richard T. Olsson [c], Figen Korel [a], Stefano Farris [b,d,*]

[a] Department of Food Engineering, Faculty of Engineering, Izmir Institute of Technology, 35430, Gülbahçe Köyü, Urla, Izmir, Turkey
[b] DeFENS, Department of Food, Environmental and Nutritional Sciences, Food Packaging Lab., University of Milan, via Celoria 2 – I, 20133, Milan, Italy
[c] Department of Fibre and Polymer Technology, School of Chemical Science and Engineering, KTH Royal Institute of Technology, Teknikringen 56, SE-100 44, Stockholm, Sweden
[d] INSTM, National Consortium of Materials Science and Technology, Local Unit University of Milan, via Celoria 2 – I, 20133, Milan, Italy

ARTICLE INFO

ABSTRACT

Developing simple, cost-effective, easy-to-use, and reliable analytical devices if of utmost importance for the food industry for rapid in-line checks of their products that must comply with the provisions set by the current legislation. The purpose of this study was to develop a new electrochemical sensor for the food packaging sector. More specifically, we propose a screen-printed electrode (SPE) modified with cellulose nanocrystals (CNCs) and gold nanoparticles (AuNPs) for the quantification of 4,4′-methylene diphenyl diamine (MDA), which is one of the most important PAAs that can transfer from food packaging materials into food stuffs. The electrochemical performance of the proposed sensor (AuNPs/CNCs/SPE) in the presence of 4,4′-MDA was evaluated using cyclic voltammetry (CV). The modified AuNPs/CNCs/SPE showed the highest sensitivity for 4,4′-MDA detection, with a peak current of 9.81 μA compared with 7.08 μA for the bare SPE. The highest sensitivity for 4,4′-MDA oxidation was observed at pH = 7, whereas the detection limit was found at 57 nM and the current response of 4,4′-MDA rose linearly as its concentration increased from 0.12 μM to 100 μM. Experiments using real packaging materials revealed that employing nanoparticles dramatically improved both the sensitivity and the selectivity of the sensor, which can be thus considered as a new analytical tool for quick, simple, and accurate measurement of 4,4′-MDA during converting operations.

1. Introduction

Primary aromatic amines (PAAs) are toxic chemicals that can transfer from food packaging materials, including polyurethane (PU) adhesives, into packaged foods. The most established route for PAAs formation in multilayer packaging materials containing aromatic PU adhesives relies on the migration of residual isocyanic monomers into the package, where they react with water molecules in the

---

package headspace. Nevertheless, for foods that have undergone thermal treatments (e.g., pasteurization and sterilization), an alternative route of PAA generation involving secondary bonds on the main PU backbone (i.e., biuret and allophanate bonds) should also be considered [1].

Risk assessment concerning the possible presence of PAAs in PU-based food packaging materials must be performed in accordance with current European regulations [2]. To this end, several analytical approaches such as spectrophotometry, chromatography, titration, electrophoresis, chemiluminescence, and fluorimetry have been successfully developed to identify and quantify PAAs. However, these approaches have several limitations. They are laborious, expensive, time-consuming, and they require large sample volumes and highly trained personnel, particularly for quality control in the food industry [3–7].

More recently, to overcome the limitations of conventional methods, smart sensors, specifically screen-printed electrochemical sensors, have attracted considerable attention owing to their ability to replace more complex techniques for detecting a wide range of substances, even in very small amounts [8]. Screen-printed electrodes (SPEs), in particular, are reliable, single-use planar devices that are produced by printing different inks on plastic, glass, or ceramic substrates [8]. The main advantage of SPEs is the miniaturization of a more complex electrochemical setup (which includes a working, reference, and counter electrode in an electrochemical cell) in one device [9]. First, this enables the use of a limited sample volume. Second, it is possible to adapt the performance of the electrode by modifying the composition of the inks/coatings on its surface according to the specific analyte to be detected. The low cost of SPEs (between 0.7 and 1.0 €/piece) allows the use of one electrode for each individual measurement so that fouling on the surface of the electrode can be avoided or at least minimized during electrochemical measurements [10,11]. Finally, in spite of their simplicity and ease of use, SPEs afford high reproducibility and sensitivity, and they do not require pre-treatment, such as electrode polishing, as other electrode materials do [12]. As for all electrochemical sensors, in SPEs the applied voltage initiates a redox reaction on the working electrode, resulting in a measurable current proportional to the concentration of the target analyte [13]. However, a bare SPE has low conductivity and low surface area, which can negatively affect the performance of the electrode. Therefore, modification of the electrode surface with metallic nanoparticles and carbon-based nanomaterials has been proposed as promising strategy to improve the electrode's surface area, electrical conductivity, and electrocatalytic properties [14–16].

In recent years, different electrochemical sensors have been developed by our group to detect PAAs. Ghaani et al. fabricated two nanosensors to quantify 2,4-diaminotoluene (TDA) and 4,4′-methylene diphenyl diamine (MDA). In these works, a glassy carbon electrode modified by different bionanocomposites of gold nanoparticles, multiwalled carbon nanotubes, and chitosan has been used as the transducer [13,15]. In another study, multiwalled carbon nanotubes and carbon mesoporous nanocomposite were used to modify a glassy carbon electrode to quantify 2,6-TDA migrating from multilayer packaging materials into food products [17]. Recently, screen-printed electrodes have gained popularity in the food industry. Hong et al. used polyethyleneimine, reduced graphene oxide, and gold nanoclusters for the detection of β-lactoglobulin in milk with high sensitivity [18]. Topsoy et al. fabricated a screen-printed electrode with a low detection limit of 2.88 nM for the quantification of diazinon [19]. Nejad et al. achieved excellent recoveries and a low limit of detection for sunset yellow detection in food using a screen-printed graphite electrode (SPGE) modified with MnO_2 nanorods anchoring graphene oxide nanocomposite [20]. Additionally, Arreguin-Campos et al. successfully applied a functionalized screen-printed electrode for the thermal detection of *E. coli* in dairy products for the first time [21]. These examples have demonstrated the potential of screen-printed electrodes to achieve accurate and sensitive detection of various compounds in the food industry.

In this work, we now attempt to translate all previous information and knowledge acquired on conventional lab-scale devices on a smaller and yet commercially-advantageous analytical devices (i.e., the SPEs). This work is the first of its kind because, based on our knowledge, there are no studies investigating SPEs specifically developed to detect PAAs. The main advantage of these novel electrodes is the higher suitability for 'in-field' applications than conventional electrodes, mainly due to a simpler cell set up. Hence, SPEs modified with appropriate nanomaterials can pave the way for sensitive, precise, easy, and in-field detection of PAAs. To this goal, a gold nanoparticles-nanocellulose hybrid nanomaterial has been used in this study to modify the surface of the SPE. The combination of AuNPs and CNCs was aimed at achieving remarkable selectivity and a low detection limit for 4,4′-MDA. The final AuNPs/CNCs/SPE was fully characterized its electrochemical properties were discussed in depth.

2. Materials and methods

2.1. Chemicals and apparatus

All the chemicals used in the present study were the same as in our previous investigations on the quantification of PAAs using conventional 'macro' electrodes, as well as the apparatuses used (i.e., the potentiostat and pH-meter) [13,15,17].

CNCs were produced according to the procedure proposed in our previous work [22], which consisted in an acid hydrolysis of bacterial cellulose obtained from *Komagataeibacter sucrofermentans* to separate the amorphous regions from the residual crystalline domains, i.e., CNCs.

2.2. Preparation of a modified screen-printed electrode

Commercial SPEs (DropSens C110, Metrohm, Herisau, Switzerland) are electrochemical sensors made of a carbon working electrode, a carbon counter electrode and a silver pseudo-reference electrode. SPEs were modified with CNCs via drop casting. A small volume (6 μL) of CNCs was cast on the working electrode surface and dried for 10 min using a double-bulb infrared light placed 40 cm far from the sample. As the last step, 4 μL of AuNPs solution were dropped on the CNCs/SP electrode to obtain the final sensor (AuNPs/

CNCs/SPE), which was then dried as previously described. For comparison purpose, CNCs/SP and AuNPs/SP electrodes were also prepared and subjected to investigation (Scheme 1).

The effective surface area of the AuNPs/CNCs/SPE was determined by cyclic voltammetry (CV) using a solution of 1.0 mM $K_3[Fe(CN)_6]$ at various scan speeds. The Randles-Sevcik formula (Eq. (1)) was used for a reversible process [23,24]:

$$I_{pa} = 2.69 \times 10^5 n^{3/2} A C_0 D^{1/2} v^{1/2} \tag{1}$$

where I_{pa} is the anodic peak current (μA), v is the scan rate (mV s^{-1}), n is the number of electrons transported, A is the electrode surface area (cm^2), D is the diffusion coefficient (cm^2 s^{-1}), and C_0 is the $K_3[Fe(CN)_6]$ concentration [23,25]. The effective mean area of the AuNPs/CNCs/SPE (0.176 ± 0.022 cm^2) was determined as the slope of I_{pa} versus $v^{1/2}$.

2.3. Surface morphology of the modified electrode

The surface of the CNCs-, AuNPs-, and AuNPs/CNCs-modified SPEs was observed by means of a field emission scanning electron microscope. The modified SPEs were first sputtered with Pt/Pd (60/40) for 20 s at a current of 80 mA under an argon atmosphere. Images were captured using a 1–5 kV acceleration voltage and a 10 μA electrode current.

2.4. Real tests on commercial multilayer packaging films

The behavior of the modified electrodes was evaluated in a real sample setting (laminate packaging materials made using PU adhesives) using the same method proposed in our previous work [15]. In brief, pouches made of three layers with a surface area of 1 dm^2 were filled with 100 mL of simulant B (acetic acid solution at 3 w/v %) and placed in an autoclave at 121 °C for 20 min.

Following the heat treatment, appropriate amounts of 4,4′-MDA were added to 20 mL simulant B/(B-R) universal buffer (1:1) mixture and detected by differential pulse voltammetry (DPV), yielding the final analyte recovery (%).

2.5. Statistical analysis

Statgraphics Plus 4.0 software (STSC, Rockville, MD, USA) was used for data analysis, whereas potential differences among samples were assessed by one-way analysis of variance. The significance level (p) was set at 0.05. Unless otherwise stated, all the analyses were performed in triplicate.
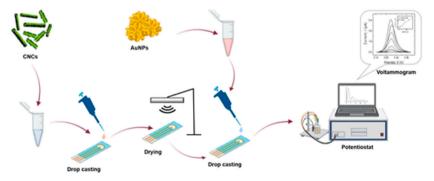
3. Results and discussion

3.1. Morphological characterization of modified SPEs

Fig. 1 shows the surface morphology of the modified electrodes as revealed by FE-SEM images. In consideration of the fact that the bare electrode surface is very smooth and the FE-SEM image thereof is represented by a flat black background (image not shown), the change in morphology arising from the modification of the bare SPE can be clearly seen. In particular, a visibly rough surface was observed in the presence of CNCs (Fig. 1a), which was due to a fibrillar, rod-shaped morphology given to the individual CNCs organized in bundles. The deposition of AuNPs led to a typical topography characterized by small nanoparticles clustered in larger domains (Fig. 1b). However, the presence of AuNPs is hardly visible when they are deposited on top of the CNCs-modified electrode most likely because they were encased in the CNCs framework (Fig. 1c).

3.2. Oxidation of 4,4′-MDA on the surface of the electrodes

CV was used to investigate the electrochemical performance of the different electrodes during the oxidation of 4,4′-MDA. Fig. 2

Scheme 1. Schematic illustration of the preparation of the AuNPs/CNCs/SPE.
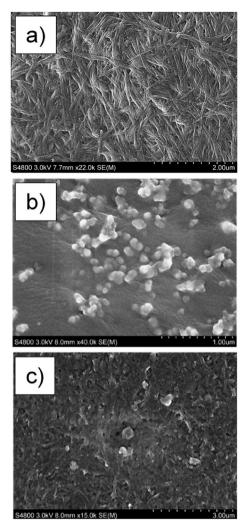
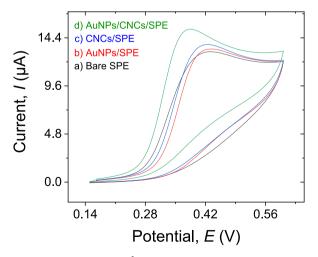**Fig. 1.** FE-SEM surface images of (a) CNCs/SPE, (b) AuNPs/SPE, (c) AuNPs/CNCs/SPE.

Fig. 2. Cyclic voltammograms in B-R buffer (pH 7.0) at a 50 mV s^{-1} scan rate of (a) bare SPE, (b) AuNPs/SPE, (c) CNCs/SPE, and (d) AuNPs/CNCs/SPE in the presence of 500 μM 4,4′-MDA.

displays the CV responses of the bare SPE, CNCs/SPE, AuNPs/SPE, and AuNPs/CNCs/SPE in the presence of 500 μM 4,4′-MDA in a Britton–Robinson (B–R) universal buffer solution (pH = 7) at a scan rate of 50 mV s^{-1}, whereas the oxidation peaks associated with each curve are reported in Table 1.

The weakest peak current response (7.08 μA) pertained to the bare electrode (Fig. 2a). The modification with only AuNPs (Fig. 2b) produced a significantly (p < 0.05) higher oxidation peak current, 7.55 μA. This finding proves that AuNPs can increase the conductivity of the SPE to a certain extent. A further improvement was observed after the modification with CNCs, which generated an oxidation peak of 7.99 μA for 4,4′-MDA at the same concentration (Fig. 2c), thus showing the greater capability of CNCs to increase the surface of the electrode compared to AuNPs, in full agreement with the micrographs of Fig. 1. Modification of the electrode with both AuNPs and CNCs yielded an additional shift of the CV plot to the highest level (Fig. 2d), which corresponded to the maximum peak current measured in this work (9.81 μA) (Table 1). The observed rise in the peak current is a clear indication of the synergistic effect that arises from the simultaneous use of CNCs and AuNPs. This effect can be likely attributed to the increased surface area and electroactivity of the modified electrode. More specifically, CNCs provide a high surface area, while the AuNPs can be thought as responsible of the high electrocatalytic activity that facilitates the electron transfer. Both higher surface area and electroactivity are crucial to increase the efficiency of the electrochemical reactions and the electrode's capacity for interaction with the analyte, respectively. Overall, the simultaneous use of CNCs and AuNPs yielded a superior electrode performance, making this approach a viable strategy for a wide range of electrochemical applications.

Interestingly, the 4,4′-MDA peak current on the bare SPE was greatly higher than the peak current recorded on a bare GCE in the presence of the same analyte [15]. The same difference was observed by Jin and co-workers when detecting dopamine using both a SPE and a GCE, which was explained in terms of differences in the working electrode structure [26,27].

However, the modification performed on the SPE resulted less effective than the modified GCE, which exhibited a maximum peak current of 25.5 μA. Plausibly, this has to be ascribed to the different modification, which included multi-walled carbon nanotubes (MWCNTs) [15], as well as to different operating conditions (e.g., pH of the test).

3.3. Effect of pH

The pH of the medium is one of the most critical factors that greatly affects the performance of a sensor, especially as far as its sensitivity is concerned. For this reason, CV tests were conducted using B-R buffer solutions with a pH ranging between 2 and 11 (Fig. 3). The highest oxidation peak current was recorded at pH = 7. As a result, all subsequent studies were carried out at this pH value. This value is lower than the optimum pH value found in our previous work [15]. However, this can be due to the different type of sensor used (GCE vs SPE), as also confirmed by Salimi et al. [28] and Huang et al. [29], who used different types of electrodes to detect dopamine. Their findings suggest that the same molecule may exhibit the best oxidation peak at different pH values depending on the electrode type and composition.

The oxidation peak potential, E_{pa}, decreased according to a quasi-linear trend (E_{pa} = −31.42 pH + 629.89; R^2 = 0.912) as the pH was increased, thus suggesting the active involvement of protons in the 4,4′-MDA oxidation reaction. According to the previously shown linear regression equation, the oxidation peak potential is shifted downward by 31.42 mV per pH unit. Based on the Nernst equation, a slope of 0.0592/2 shows a proton-to-electron ratio of 2:1, implying that one proton for every two electrons was engaged during the 4,4′-MDA oxidation.

3.4. Influence of scan rate

Fig. 4 displays the CVs of 500 μM 4,4′-MDA in B-R buffer solution at various scan rates (10–45 mV s^{-1}). The relationship between peak height (I_p) and the square root of scan rate ($\nu^{1/2}$) was linear, suggesting that, at appropriate overpotential, the process is diffusion-controlled rather than surface-controlled (Fig. 4, inset). In addition, this linear relationship indicates that no 4,4′-MDA absorption on the AuNPs/CNCs/SPE coating occurred before oxidation.

Laviron's theory, which is an appropriate technique for investigating the kinetic mechanism of the electrode with respect to the analyte, was then used in this study to gather information on the overall number of electrons (n) that took part within the electrocatalytic process. The following equation (Eq. (2)) can be thus used to calculate the anodic peak potential (E_{pa}) as a function of the natural logarithm of the scan rate (ln ν) for a completely irreversible electrode process [30]:

$$E_{pa} = E^0 + \left(\frac{RT}{\alpha n F}\right) ln\left(\frac{RTK^0}{\alpha n F}\right) + \left(\frac{RT}{\alpha n F}\right) ln\nu \qquad (2)$$

Table 1
Oxidation peak current (I_p) of 4,4′-MDA (500 μM) on the surface of different modified electrodes at pH = 7.0. Different superscript letters indicate statistical differences between the tested electrodes (p < 0.05).

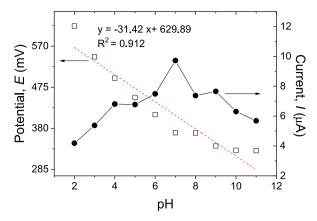| Electrode	Oxidation peak current (μA)	Drying method
Bare SPE	7.08 ± 0.06[a]	–
AuNPs/SPE	7.55 ± 0.10[b]	IR lamp
CNCs/SPE	7.99 ± 0.15[c]	IR lamp
AuNPs/CNCs/SPE	9.81 ± 0.13[d]	IR lamp

Fig. 3. Effect of pH on the oxidation peak current and potential of 4,4′-MDA (500 μM) at the AuNPs/CNCs/SPE surface. Scan rate: 50 mV s⁻¹. Electrolyte: 0.1 M B-R buffer.
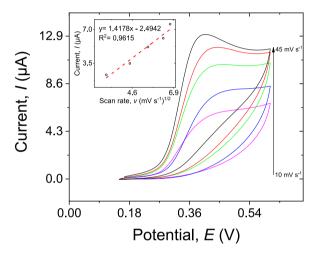

Fig. 4. Cyclic voltammograms of AuNPs/CNCs/SPE in B-R buffer (pH 7.0) including 500 μM 4,4′-MDA at various scan rates (10–45 mV s⁻¹). Inset displays the anodic peak current vs. $\nu^{1/2}$.
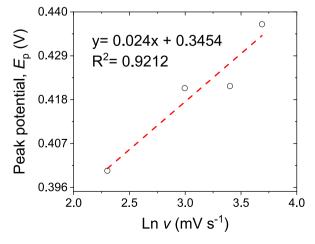

Fig. 5. Relationship between the peak potentials (E_p) and the natural logarithm of scan rates (ln ν) for 4,4′-MDA (10–40 mV s⁻¹).

where α is the transfer coefficient, n is the electron transfer number, υ is the scanning rate, E^0 is the formal redox potential, R is the gas constant (8.314 J mol^{-1} K^{-1}), T is the absolute temperature, and F is the Faraday constant (9.648 × 10^4 C mol^{-1}). It is worth noting that the elaboration of data contained in the raw voltammograms presented in Fig. 4 perfectly fit the mathematical relationship expressed by Eq. (2), thus allowing the discovery of a linear relationship between E_{pa} and ln (υ), as showed by the equation $E_p(V) =$ 0.024 ln (υ) (mV s^{-1}) + 0.3454 (Fig. 5). The slope of E_{pa} vs ln (υ), which is RT/nF, can be used to calculate the electron transfer number (n) using Laviron's equation. After the proper substitutions, the final value of n 2.14 $\approx$ 2 was achieved, which indicates that a two-electron transfer mechanism is involved in the electrochemical oxidation of 4,4'-MDA at the AuNPs/CNCs modified SPE.

3.5. Chronoamperometry measurements

To gain additional insight into the electrochemical oxidation of 4,4'-MDA on the surface of AuNPs/CNCs/SPEs, chronoamperometric studies were carried out by fixing the potential of the electrode at 550 mV and testing solutions with various concentrations of 4,4'-MDA, from 0.02 mM to 1.2 mM in B-R buffer (Fig. 6).

For an electroactive material with a diffusion coefficient D, the current response under diffusion control is described by the Cottrell equation (Eq. (3)):

$$I = \frac{nFAD^{1/2}C_b}{\pi^{1/2}t^{1/2}} \qquad (3)$$

where n is the number of electron transfers per reactant molecule which is equal to 2, F is the Faraday constant, A is the electrode effective surface area (0.176 cm^2), t is the observation time (s), C_b (mol cm^{-3}) is the concentration of 4,4'-MDA and D (cm^2 s^{-1}) is the diffusion coefficient of 4,4'-MDA.

Different linear curves were generated by plotting I against $t^{-1/2}$ for 4,4'-MDA concentrations ranging from 0.02 mM to 1.2 mM (Fig. 6a). The slope of each straight line versus 4,4'-MDA concentration allowed the total slope of the best-fit line (Fig. 6b) to be calculated using (Eq. (4)):
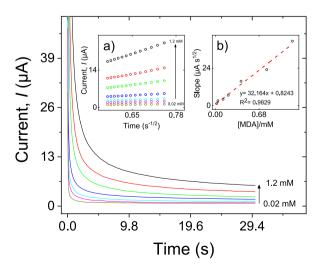
$$It^{1/2} = \frac{nFAD^{1/2}C_b}{\pi^{1/2}} \qquad (4)$$

In particular, D can thus be drawn from (Eq. (5)):

$$D = \frac{(slope)^2\pi}{(nFAC_b)^2} \qquad (5)$$

Within the Cottrell equation, the overall slope was employed to get a diffusion coefficient of 2.82 × 10^{-6} cm^2 s^{-1}. This value is lower than the coefficient of diffusion calculated in the case of a modified GCE (9.49 × 10^{-5} cm^2 s^{-1}) [15], which plausibly reflects the different mechanism of transfer due to both type of electrode and nature of the modification.

3.6. Differential pulse voltammetric studies

In this work, the sensitivity of the AuNPs/CNCs screen-printed electrode to 4,4'-MDA was investigated by differential pulse

Fig. 6. Chronoamperograms obtained at AuNPs/CNCs/SPE in B-R buffer solution (pH 7.0) for various 4,4'-MDA concentrations (0.02–1.2 mM). Insets: (a) plots of I vs. $t^{-1/2}$ gained from the chronoamperograms. (b) plot of the slope of the straight lines against 4,4'-MDA concentration.

voltammetry (DPV).

To obtain the DP voltammograms of 4,4′-MDA, appropriate volumes of the stock solutions of 4,4′-MDA were added to the cell containing B-R buffer (9 mL) for a total volume of 10 mL. Fig. 7 shows the voltammetric response of 4,4′-MDA at different concentrations. The calibration curve of 4,4′-MDA was linear across a single concentration range (0.12–100 μM) (inset of Fig. 7). The proposed sensor's lower limit of detection (LOD) was computed using the equation below (Eq. (6)):

$$LOD = (3 \times S_{bl}) / m \tag{6}$$

where the slope of the linear range in the voltammetric plot (m) was 0.0576 A (M)$^{-1}$ and S_{bl} is the standard deviation of the current response (μA) derived from the blank solution (10 replicates). Eventually, the AuNPs/CNCs/SPE LOD value was calculated to be 0.057 μM.

A comparison of our work with the study carried out by Ghaani et al. shows that the modified GCE had a lower LOD than the modified SPE of this study (AuNPs/CNCs/SPE) [15], somehow in line with our previous observations on the higher performance of a GCE system. As reported in the literature, a higher LOD of modified SPEs compared to modified GCEs was confirmed by other authors. For example, the LOD of a GCE modified with MWCNTs-AuNPs for bisphenol A was 7.5 nM [31], while the LOD of a magnetic-activated carbon-cobalt modified SPE for the same analyte was 10 nM [32]. Jin et al. found a LOD of 20 nM for the dopamine detection using a poly (p-aminobenzene sulfonic acid)-modified GCE [26], whereas Moreno et al. calculated a LOD of 60 nM for dopamine on graphene quantum dots/ionic liquid-modified SPE [27]. Interestingly, both a GCE and a SPE with the same modification were used for the detection of catechol [33,34]. LOD values were found at 41 nM and 100 nM, respectively. Accordingly, GCEs seem to achieve a lower detection limit than SPEs.

3.7. Interference study

Interference effects generated by the simultaneous presence of electroactive compounds in the target solution can affect adversely the performance of the sensor. In the case of multilayer packaging materials, a variety of additives are added to the films during the extrusion process. These additives can migrate from the films thus decreasing the electrode performance toward the target analyte. As a result, in this study we examined the electrocatalytic efficacy of the AuNPs/CNCs/SPE against 4,4′-MDA in the presence of a variety of possibly interfering chemicals.

The modified screen-printed was tested against two additives commonly used in polyolefins, namely Irganox® 1010 and Irgafos® 168, which are used as antioxidant and processing stabilizer, respectively. DPV experiments (data not shown) revealed that no increase in the current response was observed after the addition of these compounds (40 μM) to the 4,4′-MDA containing solution, demonstrating that the fabricated sensor is suitable for selective 4,4′-MDA detection.

Lastly, a relative standard deviation (RSD) of 3.65% was obtained when a single modified electrode (AuNPs/CNCs/SPE) was used for five consecutive measurements in the same 4,4′-MDA solution (10 μM), hence demonstrating the high performance of the sensor in terms of repeatability. Similarly, the reproducibility of the proposed sensor was investigated through DP voltammograms at 10 μM 4,4′-MDA using five independent distinct sensors of the same configuration (AuNPs/CNCs/SPE). The measured RSD (4.20%) indicates good reproducibility of the fabricated sensor.

3.8. Real sample analysis

The AuNPs/CNCs/SP electrode was also tested for its capability to detect and quantify 4,4′-MDA in real sample experiments. For this reason, food simulant B (3 w/v % acetic acid water solution) was employed within a pouch that was subsequently subjected to 121 °C for 20 min (sterilization conditions). The conventional addition model was used to evaluate the modified electrode's ability to detect 4,4′-MDA. As can be seen in Table 2, the AuNPs/CNCs-modified electrode worked efficiently, with high recovery (98.20–104.07%). This result clearly shows that the AuNPs/CNCs/SPE may be utilized to detect 4,4′-MDA migration from multilayer packages that have been subjected to thermal stresses. SPE's recovery was slightly higher than GCE's, which is consistent with other studies [15,31,32].

4. Conclusions

In this work, the detection of 4,4′-MDA, one of the most hazardous PAAs that might contaminate foods by migrating from multilayer PU adhesive-based packaging materials, was proposed by developing a new screen-printed electrode modified with CNCs and AuNPs. The simultaneous use of CNCs and AuNPs was highlighted as the main reason for superior sensitivity of the modified sensor over the bare SPE as far as the electro-oxidation of 4,4′-MDA was concerned. This work demonstrated the excellent analytical performance of the modified SPE towards 4,4′-MDA, especially at pH 7.0, whereby the electrode exhibited a limit of detection of 0.057 μM and a linear detection range from 0.12 to 100 μM of 4,4′-MDA, with simultaneous satisfactory repeatability and reproducibility. For these reasons, the proposed sensor could be a viable alternative to conventional analytical instrumentation used for the detection of PAAs, particularly for quality control in converting operations of the food packaging industry.
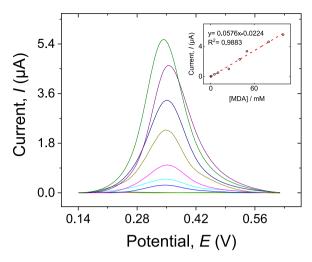
Fig. 7. Differential pulse voltammetry response of AuNPs/CNCs/SPE in 10 mL B-R buffer (pH = 7.0) containing different concentrations of 4,4′-MDA (0.12–100 μM). The peak current against 4,4′-MDA concentration is shown in the inset of the plot.

Table 2
Amount of added (spiked) and measured 4,4′-MDA at the AuNPs/CNCs/SPE surface, with resulting recovery percentage after the migration test using the acidic food simulant (simulant B) under typical sterilization conditions (121 °C for 20 min).

Sample	Spiked (μM)	Found (μM)	Recovery (%)
Laminate structure (PET/EVOH/PE) including a PU adhesive	0	–	–
	5	4.91	98.20
	40	41.63	104.07
	80	79.02	98.77

Declarations

Author contribution statement

Duygu Büyüktaş, Masoud Ghaani: Conceived and designed the experiments; Performed the experiments; Analyzed and interpreted the data; Wrote the paper.

Cesare Rovera: Conceived and designed the experiments; Wrote the paper.

Daniele Carullo: Analyzed and interpreted the data; Wrote the paper.

Richard T. Olsson: Performed the experiments; Contributed reagents, materials, analysis tools or data.

Figen Korel: Contributed reagents, materials, analysis tools or data; Wrote the paper.

Stefano Farris: Conceived and designed the experiments; Contributed reagents, materials, analysis tools or data; Analyzed and interpreted the data; Wrote the paper.

Data availability statement

Data will be made available on request.

Declaration of interests statement

The authors declare no conflict of interest.

Additional information

No additional information is available for this paper.

References

[1] G. Campanella, M. Ghaani, G. Quetti, S. Farris, On the origin of primary aromatic amines in food packaging materials, Trends Food Sci. Technol. 46 (2015) 137–143, https://doi.org/10.1016/j.tifs.2015.09.002.

[2] European Commission, Commission Regulation (EU), No. 10/2011 of 14 January, 2011, Off, Off. J. Eur. Union 54 (2011) 1–89.

[3] C. Brede, I. Skjevrak, Migration of aniline from polyamide cooking utensils into food simulants, Food Addit. Contam. 21 (2004) 1115–1124, https://doi.org/10.1080/02652030400019349.

[4] M. Mattarozzi, F. Lambertini, M. Suman, M. Careri, Liquid chromatography–full scan-high resolution mass spectrometry-based method towards the comprehensive analysis of migration of primary aromatic amines from food packaging, J. Chromatogr. A 1320 (2013) 96–102, https://doi.org/10.1016/j.chroma.2013.10.063.

[5] X. Wang, Y. Chen, Determination of aromatic amines in food products and composite food packaging bags by capillary electrophoresis coupled with transient isotachophoretic stacking, J. Chromatogr. A 1216 (2009) 7324–7328, https://doi.org/10.1016/j.chroma.2009.05.089.

[6] N. Chen, L. Chen, Y. Cheng, K. Zhao, X. Wu, Y. Xian, Molecularly imprinted polymer grafted graphene for simultaneous electrochemical sensing of 4, 4-methylene diphenylamine and aniline by differential pulse voltammetry, Talanta 132 (2015) 155–161, https://doi.org/10.1016/j.talanta.2014.09.008.

[7] A. Rehman, N. Iqbal, P.A. Lieberzeit, F.L. Dickert, Multisensor biomimetic systems with fully artificial recognition strategies in food analysis, Monatsh. Chem. 140 (2009) 931–939, https://doi.org/10.1007/s00706-009-0151-5.

[8] P. Masawat, J.M. Slater, The determination of tetracycline residues in food using a disposable screen-printed gold electrode (SPGE), Sensor. Actuator. B Chem. 124 (2007) 127–132, https://doi.org/10.1016/j.snb.2006.12.010.

[9] R.O. Kadara, B.G. Haggett, B.J. Birch, Disposable sensor for measurement of vitamin B2 in nutritional premix, cereal, and milk powder, J. Agric. Food Chem. 54 (2006) 4921–4924, https://doi.org/10.1021/jf0603376.

[10] O.D. Renedo, M.A. Alonso-Lomillo, M.A. Martínez, Recent developments in the field of screen-printed electrodes and their related applications, Talanta 73 (2007) 202–219, https://doi.org/10.1016/j.talanta.2007.03.050.

[11] W.Y. Su, S.M. Wang, S.H. Cheng, Electrochemically pretreated screen-printed carbon electrodes for the simultaneous determination of aminophenol isomers, J. Electroanal. Chem. 651 (2011) 166–172, https://doi.org/10.1016/j.jelechem.2010.11.028.

[12] J.P. Metters, R.O. Kadara, C.E. Banks, New directions in screen printed electroanalytical sensors: an overview of recent developments, Analyst 136 (2011) 1067–1076, https://doi.org/10.1039/C0AN00894J.

[13] M. Ghaani, C. Rovera, F. Pucillo, M.R. Ghaani, R.T. Olsson, M. Scampicchio, S. Farris, Determination of 2,4-diaminotoluene by a bionanocomposite modified glassy carbon electrode, Sensor. Actuator. B Chem. 277 (2018) 477–483, https://doi.org/10.1016/j.snb.2018.09.053.

[14] B.L. Hanssen, S. Siraj, D.K. Wong, Recent strategies to minimise fouling in electrochemical detection systems, Rev. Anal. Chem. 35 (2016) 1–28, https://doi.org/10.1515/revac-2015-0008.

[15] M. Ghaani, F. Pucillo, R.T. Olsson, M. Scampicchio, S. Farris, A bionanocomposite-modified glassy carbon electrode for the determination of 4, 4′-methylene diphenyl diamine, Anal. Methods 10 (2018) 4122–4128, https://doi.org/10.1039/c8ay01376d.

[16] S. Viswanathan, J. Radecki, Nanomaterials in electrochemical biosensors for food analysis - a review, Pol. J. Food Nutr. Sci. 58 (2008) 157–164.

[17] D. Büyüktaş, M. Ghaani, C. Rovera, R.T. Olsson, F. Korel, S. Farris, Development of a nano-modified glassy carbon electrode for the determination of 2,6-diaminotoluene (TDA), Food Packag. Shelf Life 29 (2021) 100714, https://doi.org/10.1016/j.fpsl.2021.100714.

[18] J. Hong, Y. Wang, L. Zhu, L. Jiang, An electrochemical sensor based on gold-nanocluster-modified graphene screen-printed electrodes for the detection of β-Lactoglobulin in milk, Sensors 20 (2020) 3956, https://doi.org/10.3390/s20143956.

[19] O.K. Topsoy, F. Muhammad, S. Kolak, A. Ulu, Ö. Güngör, M. Şimşek, S. Köytepe, B. Ateş, Fabrication of electrospun polycaprolactone/chitosan nanofiber-modified screen-printed electrode for highly sensitive detection of diazinon in food analysis, Measurement 187 (2022), 110250, https://doi.org/10.1016/j.measurement.2021.110250.

[20] F.G. Nejad, M.H. Asadi, I. Sheikhshoaie, Z. Dourandish, R. Zaimbashi, H. Beitollahi, Construction of modified screen-printed graphite electrode for the application in electrochemical detection of sunset yellow in food samples, Food Chem. Toxicol. 166 (2022), 113243, https://doi.org/10.1016/j.fct.2022.113243.

[21] R. Arreguin-Campos, M. Frigoli, M. Caldara, R.D. Crapnell, A.G.M. Ferrari, C.E. Banks, T.J. Cleij, H. Diliën, K. Eersels, B. van Grinsven, Functionalized screen-printed electrodes for the thermal detection of Escherichia coli in dairy products, Food Chem. 404 (2023), 134653, https://doi.org/10.1016/j.foodchem.2022.134653.

[22] C. Rovera, M. Ghaani, N. Santo, S. Trabattoni, R.T. Olsson, D. Romano, S. Farris, Enzymatic hydrolysis in the green production of bacterial cellulose nanocrystals, ACS Sustain. Chem. Eng. 6 (2018) 7725–7734, https://doi.org/10.1021/acssuschemeng.8b00600.

[23] A.J. Bard, L.R. Faulkner, Electrochemical Methods: Fundamentals and Applications, second ed., John Wiley & Sons, New York, 2001.

[24] N. Nasirizadeh, H.R. Zare, A.R. Fakhari, H. Ahmar, M.R. Ahmadzadeh, A. Naeimi, A study of the electrochemical behavior of an oxadiazole derivative electrodeposited on multi-wall carbon nanotube-modified electrode and its application as a hydrazine sensor, J. Solid State Electrochem. 15 (2011) 2683–2693, https://doi.org/10.1007/s10008-010-1259-6.

[25] N. Nasirizadeh, Z. Shekari, H.R. Zare, S. Makarem, Electrocatalytic determination of dopamine in the presence of uric acid using an indanedione derivative and multiwall carbon nanotubes spiked in carbon paste electrode, Mater. Sci. Eng. C 33 (2013) 1491–1497, https://doi.org/10.1016/j.msec.2012.12.051.

[26] G. Jin, Y. Zhang, W. Cheng, Poly (p-aminobenzene sulfonic acid)-modified glassy carbon electrode for simultaneous detection of dopamine and ascorbic acid, Sensor. Actuator. B Chem. 107 (2005) 528–534, https://doi.org/10.1016/j.snb.2004.11.018.

[27] M. Moreno, A.S. Arribas, E. Bermejo, M. Chicharro, A. Zapardiel, M.C. Rodríguez, G.A. Rivas, Selective detection of dopamine in the presence of ascorbic acid using carbon nanotube modified screen-printed electrodes, Talanta 80 (2010) 2149–2156, https://doi.org/10.1016/j.talanta.2009.11.022.

[28] A. Salimi, H. MamKhezri, R. Hallaj, Simultaneous determination of ascorbic acid, uric acid and neurotransmitters with a carbon ceramic electrode prepared by sol–gel technique, Talanta 70 (2006) 823–832, https://doi.org/10.1016/j.talanta.2006.02.015.

[29] D.Q. Huang, C. Chen, Y.M. Wu, H. Zhang, L.Q. Sheng, H.J. Xu, Z.D. Liu, The determination of dopamine using glassy carbon electrode pretreated by a simple electrochemical method, Int. J. Electrochem. Sci. 7 (2012) 5510–5520.

[30] E. Laviron, Adsorption, autoinhibition and autocatalysis in polarography and in linear potential sweep voltammetry, J. Electroanal. Chem. Interfacial Electrochem. 52 (1974) 355–393, https://doi.org/10.1016/S0022-0728(74)80448-1.

[31] X. Tu, L. Yan, X. Luo, S. Luo, Q. Xie, Electroanalysis of bisphenol A at a multiwalled carbon nanotubes-gold nanoparticles modified glassy carbon electrode, Electroanalysis 21 (2009) 2491–2494, https://doi.org/10.1002/elan.200900195.

[32] F. Emambakhsh, H. Asadollahzadeh, N. Rastakhiz, S.Z. Mohammadi, Highly sensitive determination of Bisphenol A in water and milk samples by using magnetic activated carbon–Cobalt nanocomposite-screen printed electrode, Microchem. J. 179 (2022), 107466, https://doi.org/10.1016/j.microc.2022.107466.

[33] D. Talarico, F. Arduini, A. Constantino, M. Del Carlo, D. Compagnone, D. Moscone, G. Palleschi, Carbon black as successful screen-printed electrode modifier for phenolic compound detection, Electrochem. Commun. 60 (2015) 78–82, https://doi.org/10.1016/j.elecom.2015.08.010.

[34] M.M. Lounasvuori, D. Kelly, J.S. Foord, Carbon black as low-cost alternative for electrochemical sensing of phenolic compounds, Carbon 129 (2018) 252–257, https://doi.org/10.1016/j.carbon.2017.12.020.